Biosensors and Bioelectronics 24 (2009) 1405–1410

Contents lists available at ScienceDirect

Biosensors and Bioelectronics

journal homepage: www.elsevier.com/locate/bios

Nano-silver-modified PQC/DNA biosensor for detecting *E. coli* in environmental water

H. Sun [a], T.S. Choy [a], D.R. Zhu [a], W.C. Yam [b], Y.S. Fung [a,*]

[a] *The Department of Chemistry, The University of Hong Kong, Hong Kong SAR, China*
[b] *The Department of Microbiology, The University of Hong Kong, Hong Kong SAR, China*

ARTICLE INFO

Article history:
Received 6 May 2008
Received in revised form 24 July 2008
Accepted 5 August 2008
Available online 13 August 2008

Keywords:
Biosensor
Piezoelectric quartz crystal
E. coli
PCR
Ag
TiO_2

ABSTRACT

To meet the requirement of World Health Organization for zero tolerance of *E. coli* cell in 100 mL drinking water, a new procedure based on photodeposition of nano-Ag at TiO_2-coated piezoelectric quartz crystal (PQC) electrode was developed to fabricate a highly sensitive PQC/DNA biosensor. Enhancement of 3.3 times for binding of complementary DNA has been shown and attributed to the following effects arising from the nano-Ag coating. First, a large increase in the active surface area and packing density of neutravidin enhances the maximum neutravidin load to 1.8 times of a normal electrode. Second, the functional activity of neutravidin is enhanced by chemical interaction with nano-Ag to give rise to an increase in the binding ratio between neutravidin and biotinylated DNA probe from 1.00:1.76 to 1.00:3.01. Third, the stronger binding leads to a higher stability of the biotinylated DNA probes bound and increase in hybridization with the complementary DNA. Under the optimized conditions for flow analysis with online PCR product denaturing and hybridization, a detection limit of eight *E. coli* cells are obtained which require sampling at least 800 mL water to detect a single *E. coli* cell in 100 mL water.

1. Introduction

For public health protection against bacterial infection of drinking water, monitoring of bacteria is needed. The use of *E. coli* is recommended by the World Health Organization (WHO) as the first choice bacterial indicator for routine analysis (Guideline Values for Drinking Water, 2004), requiring the detection of zero *E. coli* cell in any 100-mL drinking water collected during inspection. Although existing microbiological techniques based on morphological evaluation allow the detection of low-bacteria count, it requires the growth of cells into colonies, a time-consuming procedure demanding 24–48 h for presumptive results and a further 48 h for confirmation.

To enable a quick detection of *E. coli* during emergency monitoring, DNA hybridization techniques had been developed with detection by electrochemical (Loaiza et al., 2007; Arora et al., 2007), optical (Kim et al., 2007; Hwang et al., 2006), and microgravimetric methods based on piezoelectric quartz crystal (PQC) sensing (Wu et al., 2007; Mao et al., 2006). Compared to electrochemical and optical methods, the PQC biosensor provides a label-free detection method using simple and portable equipment setup, hence offering a high potential for direct detection of *E. coli* in field application as shown in our recent results with a detection limit for 23 *E. coli* cells (Sun et al., 2006).

Various methods (Hoshino et al., 2006; Ogi et al., 2006; Caruso et al., 1997) utilizing PQC with high-resonance frequency, sensing coatings with multi-layers of DNA-containing films or various post-signal amplification strategies (Chu et al., 2006; Fu, 2008; Mao et al., 2006; Su and Li, 2005) had been used to enhance the sensitivity of PQC biosensor. However, frequency stability problems are encountered using PQC with resonance frequencies higher than 10 MHz and complicate procedures have to be used in multi-layer immobilization and post-signal amplification. In addition, their operations are expensive and require critically controlled working conditions, hence not suitable for direct environmental monitoring of *E. coli*.

A more practical approach is to increase the amount of active recognition molecules at the surface of the PQC biosensor to facilitate the capturing of analyte DNA. It is critically important to increase the surface area and biocompatibility of PQC electrode to enhance avidin/neutravidin loading, improve the functional activity of the sensing layer and maintain a good stability of the analyte signal. Thus, procedures had been developed to incorporate gold nanoparticles onto the biosensing layer to enhance detection sensitivity using various cross-linkers such as 1,6-hexanedithiol (Fu et al., 2007; Sivanesan et al., 2007), cysteamine (Manso et al., 2008; Shervedani and Bagherzadeh, 2008) and cystamine monolayer (Raj et al., 2005; Zhang et al., 2005). The procedure is laborious and uses

* Corresponding author. Tel.: +852 28592162; fax: +852 25482132.
E-mail address: ysfung@hkucc.hku.hk (Y.S. Fung).

0956-5663/$ – see front matter © 2008 Elsevier B.V. All rights reserved.
doi:10.1016/j.bios.2008.08.008

many manipulation steps. In addition, the coating layer of nano-Au can be detached from the electrode surface during storage. Thus, the procedure is not suitable to deposit a controllable amount of coating at the PQC electrode surface.

Due to the higher reactivity of silver, Ag nanoparticles had been produced by in situ deposition onto the PQC electrode surface via evaporation, electrochemical and photochemical method (Chen et al., 2007; Friedmann et al., 2007; Sun et al., 2005). The evaporation method requires special coating equipment and electrochemical methods require critical control of various working parameters to reduce side reaction and produce nano-Ag particles with narrow particle size distribution. No report has been found in the literature using photochemical method to deposit nano-Ag onto PQC electrode surface for DNA biosensor application. This approach is explored to fabricate a suitable sensing layer for the PQC/DNA biosensor to detect *E. coli* in drinking water. Results on the optimized working conditions for detecting *E. coli* PCR products under flow analysis with online PCR product denaturing prior to hybridization are given and discussed with regards to its applicability for determining *E. coli* in drinking water.

2. Experimental

2.1. Material and reagents

Neutravidin was purchased from Pierce Biotechnology Inc. (Rockford, USA), whereas 1,6-hexanedithiol [$HS(CH_2)_6SH$], Agarose gel powders, Tris and other reagents from Sigma–Aldrich Inc. (St. Louis, USA), Biotinylated ssDNA probe, primers UAL-1939 and UAR-2105 and other oligonucleotides from Tech Dragon Limited (Hong Kong); dNTP (deoxynucleoside triphosphate) mix, 10 × PCR buffer II (including 100 mM Tris–HCl, 500 mM KCl, pH 8.3) and Gold Taq DNA polymerase from Applied Biosystems (Foster, USA); ΦX174 DNA/BsuRI (HaeIII) markers from Fermentas Life Sciences (Hanover, USA) and titanium dioxide (TiO_2) (surface area 50 cm^2/g and density 3.8 g/cm^3) from Degussa (P25, ca. 80% anatase and 20% rutile). The colloidal gold nano-particles were prepared according to literature procedure (Zhong et al., 2004).

2.2. Apparatus and equipment

PCR amplification was performed in a GeneAmp PCR System 9700 (Applied Biosystems, Foster, USA). An electrophoresis system (model DYY-5, Liuyi Instrument Factory, Beijing, China) was used to conduct gel electrophoresis with electropherograms recorded by an UV trans-illuminator (Bio-Rad Mini Trans-Illuminator) with a Polaroid Direct Screen Instant Camera (Polaroid, UK). The 9 MHz AT-cut quartz crystals (12.5 mm diameter) with gold deposited (28.3 mm^2 area) on both sides were obtained from CH Instruments Inc. (Shanghai, China). The quartz crystal was placed inside a methacrylate housing with only one side in contact with the solution. A self-constructed oscillator circuit powered by a 5 V DC voltage regulator was used to resonate PQC with frequency output monitored by a frequency counter (Heathkit model IM-4120). The electrochemical impedance spectrum was taken by the CHI 760B system (CH Instruments Inc., Shanghai, China) in an electrochemical cell with a three-electrode configuration (9 MHz Au-PQC working electrode; Ag/AgCl reference electrode and Pt counter electrode) in electrolyte containing 0.2 mol/L NaCl, 1 mmol/L $K_4Fe(CN)_6$, 1 mmol/L $K_3Fe(CN)_6$, and 0.05 mol/L Na_2HPO_4 at pH 7.5. The UV lamp was purchased from Spectroline (Model EF-140C/F) and the Scanning Electron Microscope micrographs from Cambridge Leica (Model Stereo Scan 440).

2.3. Procedures

Genomic DNA of *E. coli* (ACTT 25922) was extracted (Leung et al., 2001) and the 25-μL PCR mixture contained 3 μL of DNA extract, 1 μM of each primer, 0.2 mM of each dNTP, 1.5 mM $MgCl_2$ and 1.25 units Gold Taq polymerase. The target DNA was amplified using an initial denaturation at 95 °C for 5 min and then 50 PCR cycles of the three-step PCR amplification (denaturation at 95 °C for 15 s, primer reannealing at 50 °C for 30 s and primer extension at 72 °C for 30 s). A final elongation was carried out at 72 °C for 7 min, following by a final cooling stage at 4 °C before post-PCR analysis.

The self-assembly method (Liu et al., 2004) was used to immobilize nano-Au particles onto the PQC electrode by firstly immersing it into a 0.5% (v/v) 1,6-hexanedithiol solution in ethanol for 30 min, following by immobilization in an aqueous Au colloidal solution for 1 h at room temperature. To prepare the TiO_2-coated PQC electrode, the gold-plated surface was firstly washed with $K_2Cr_2O_7$–conc. H_2SO_4 (1:30, g/g) solution for 2 min and then distilled water thoroughly. Aqueous TiO_2 solution (0.5%) was then added dropwise onto the quartz crystal surface prior to drying in air. Before and after TiO_2 coating, the quartz crystal frequencies were monitored to estimate coating thickness. After heating at 100 °C for 1 h, the films were sintered at 450 °C for 20 min to produce a stable microcrystalline TiO_2 film. For photochemical deposition of nano-Ag particles, the TiO_2-coated PQC electrode was immersed into a 10^{-2} mol/L $AgNO_3$ solution (10%, v/v methanol in water) under irradiation by an UV lamp at 380 nm for 20 min with in situ frequency monitoring.

For DNA analysis, the TRIS buffer (10 mM Tris, 1 mM EDTA, 0.2 M NaCl, pH 7.5) was initially pumped to the detection cell till a stable baseline was obtained. 20 μL of neutravidin (1 mg/mL) was then injected, following by 20 min waiting period with pump stopping. After washing and filling with buffer (100 μL), 15 μL biotinylated probe (15 μg/mL) was injected, following by 20 min waiting period before washing and filling again using 100 μL buffer. 20 μl PCR products were then pumped firstly at a slow flow (0.02 mL/min) through the hot coiled tubing at 100 °C for 5 min and then rapidly into the cold coiled tubing at 0 °C for 2 min before a rapid transfer (flow at 10 mL/min) to the detection cell. After the injection of all denatured PCR products for 15 min, the cell was washed again with the buffer until the frequency was stable before recording the frequency shifts. To regenerate the neutravidine/biotinylated probe modified electrode, 1 mM HCl was added to the electrode surface for 30 s, following by a thorough washing using the buffer solution.

3. Results and discussion

3.1. Preparation and characterization of TiO_2 coating at PQC surface

The TiO_2 coating at the PQC electrode surface was prepared by literature procedure (Tao et al., 2004). A total frequency shift of about 10,000 Hz was obtained, attributed to the formation of a layer of TiO_2 at the PQC electrode surface. The thickness of the TiO_2 layer was estimated to be about 0.15 μm according to the Sauerbrey equation (Sauerbrey, 1959). To characterize the microcrystalline TiO_2 film, the electrochemical impedance spectra (EIS) were recorded with the associated Nyquist plots shown in Fig. 1. The Z_{re} and Z_{im} shown represent the real and imaginary part of the impedance, respectively. The Nyquist plot can be divided into a low-frequency range controlled by diffusion and a high-frequency range limited by electrode kinetics. Using a bare PQC electrode, a straight line (plot a of Fig. 1) is obtained for the entire frequency range, indicating that the reaction is mainly controlled by diffusion and

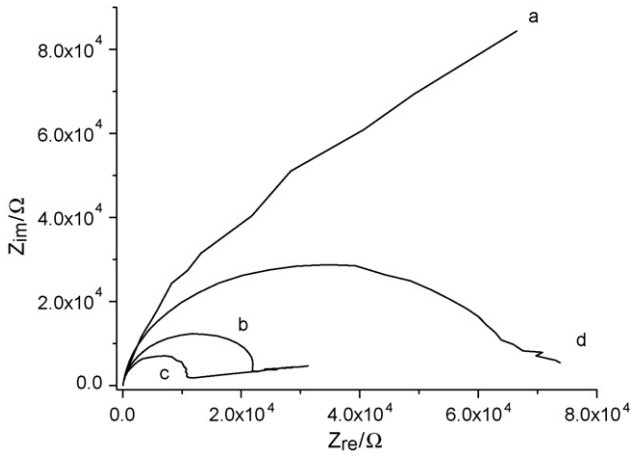

Fig. 1. Electrochemical impedance spectra of (a) normal PQC electrode; (b) TiO_2-coated PQC electrode; (c) nano-Ag/TiO_2-coated PQC electrode; (d) neutravidin-modified nano-Ag/TiO_2-coated PQC electrode. Initial E (V) = −0.2; high frequency (Hz) = 10^5; low frequency (Hz) = 0.005; amplitude (V) = 0.005; quiet time (s) = 2; cycles (0.1–1 Hz) = 1; cycles (0.01–0.1 Hz) = 1; cycles (0.001–0.01 Hz) = 1.

not limited by electron transfer at the electrode surface. Whereas an arc in the high-frequency range and a line in the low-frequency range are observed for the TiO_2-modified PQC electrode (plot b of Fig. 1). The diameter of the semicircle with the Z_{re}-axis is equal to R_{et} (interfacial electron-transfer resistance) and its increase reflects the corresponding change in the resistance due to the formation of an insulating layer at the surface of the PQC electrode. The R_{et} is calculated to be about 22,135 Ω, indicating that the semiconductor TiO_2 film is completely covering the entire electrode surface, leading to a drastic increase in the electron-transfer resistance and the production of a suitable surface for subsequent photochemical formation of nano-Ag particles.

3.2. *In situ photochemical formation of nano-Ag particles at TiO_2-coated PQC surface*

The effect of methanol on the photodeposition of Ag is shown in Fig. 2. The photodeposition rate is found to increase with methanol concentration in the $AgNO_3$ solution. The response reaches a plateau when methanol is higher than 5%. To obtain a repeatable amount of Ag deposited, 10% (v/v) methanol was added to the

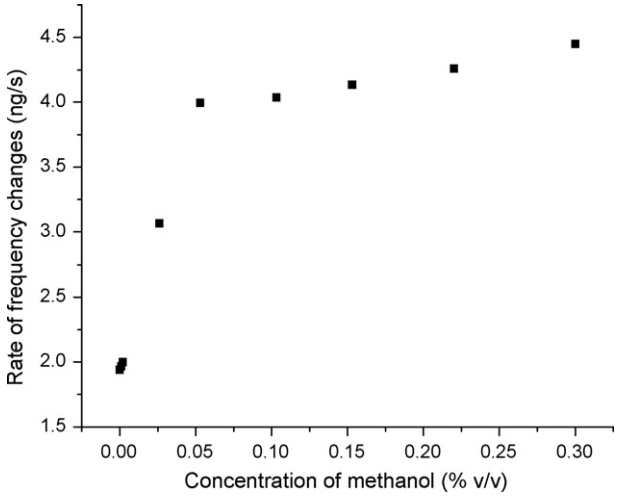

Fig. 2. The effect of methanol on the photo-reduction of silver in 0.01 M $AgNO_3$ aqueous solution.

$AgNO_3$ solution. The total amount of photodeposited nano-Ag particles and their associated morphology are found highly dependent on the $AgNO_3$ concentration. The morphological features shown in the SEM micrographs (Fig. 3) indicate the production of nano-silver particles with wide size distribution in isolated areas at the electrode surface when $AgNO_3$ is10^{-4} M (Fig. 3(B)). A coating with full coverage of nano-silver is obtained when $AgNO_3$ is increased to 10^{-3} M (Fig. 3(C)). Further increase to 10^{-2} M leads to smaller nano-Ag particles with narrow size distribution covering the entire electrode surface (Fig. 3(D)). This indicates that the deposition is mainly controlled by nuclei formation at the initial stage of photochemical formation until a complete nano-Ag layer is formed.

As nano-Ag particles with smaller sizes possess a large surface area favorable for subsequent modification using neutravidin, 10^{-2} M of $AgNO_3$ is used for photo-deposition of nano-Ag. Metallic silver is observed to appear at electrode surface during irradiation as indicated by a visual change in color from white to brown. After photodeposition of nano-Ag onto the TiO_2-coated PQC electrode, the diameter of the arc in the EIS Nyquist plot (plot c in Fig. 1) decreases obviously with corresponding reduction of R_{et} to 10,736 Ω and an increase in the conductivity of the electrode, which is attributed to the production of a metallic nano-Ag layer at the PQC electrode surface.

3.3. *Modification of the nano-Ag/TiO_2/PQC electrode with neutravidin and biotinylated ssDNA probes*

A commonly used diagnostic DNA method for *E. coli* determination is to detect its *uid* gene directly. As the carboxyl end of the *uid A* gene has been reported to be unique and conserved in general *E. coli* (Iqbal et al., 1997), a structural region (166 bp) located at the carboxyl coding region of the *uid A* gene is selected to be amplified by PCR. The sequence of the biotinylated ssDNA probe is targeted at locations close to the end of the amplified 166-bp gene fragment. This design facilitates the placement of the probe to its complementary sequence in the long gene fragment and overcomes to some extent the stereochemical and orientational hindrance to improve the hybridization efficiency. The sequence of the PCR products, probes and oligonuleotides are listed in Table 1.

The use of nano-Au-modified PQC electrode has shown (Table 2) to improve the maximum frequency response for neutravidin and biotinylated DNA probes as compared to normal PQC electrode (350 and 82 Hz vs. 310 and 53 Hz, respectively). However, the best performance is using nano-Ag-modified PQC electrode with the highest frequency response for neutravidin and biotinylated DNA probe (556 and 162 Hz, respectively) as well as the largest reagent loading. In addition, a bigger noise has been observed during modification and detection using nano-Au PQC sensor.

Under the optimum conditions, the maximum frequency responses (ΔF_{sol} in solution) due to neutravidin immobilization are 556 and 310 Hz using nano-Ag-modified and normal PQC electrode, respectively. To calculate the mass of neutravidin adsorbed onto the PQC electrode surface, the ΔF_{sol} value cannot be used directly due to the presence of water within the adsorbed layer, the viscoelastic effects arising at the boundary between the solvent and the adsorbed layer, as well as the slip between the film and substrate (Ghafouri and Thompson, 1999). The average frequency shift in air (ΔF_{air}) due to the absorption of neutravidin is 270 Hz at the nano-Ag-modified electrode, which is about half of ΔF_{sol}. For an AT-cut 9 MHz PQC electrode, a change of 1 Hz in air corresponds to a mass change of 5.5 ng/cm^2 at the surface of the crystal according to the Sauerbrey theory. Thus, the packing density of neutravidin onto the nano-Ag-modified PQC electrode is estimated as 2.48×10^{-11} mol cm^{-2}. Similar calculation for normal PQC electrode produces a packing density of neutravidin as

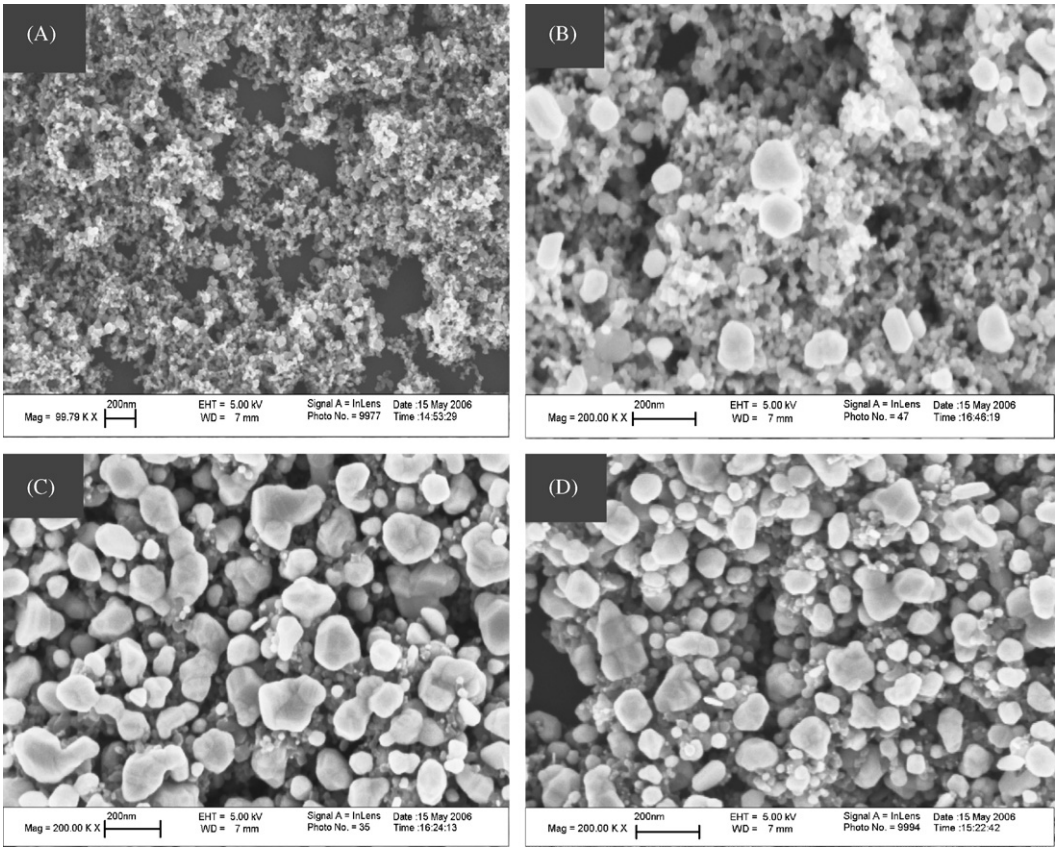

Fig. 3. The SEM micrographs showing the surface features of TiO_2-coated PQC electrodes (A) before immersion; and after immersion under 20 min UV illumination in (B) 10^{-4} M $AgNO_3$, (C) 10^{-3} M $AgNO_3$ and (D) 10^{-2} M $AgNO_3$.

Table 1
The sequence of various oligonucleotides, primers and PCR product utilized in the present study.

Oligonucleotides	Sequence[a]
Biotinylated ssDNA probe	5′-Biotin-CAAAAACGCTGGACTGGC-3′
Complementary DNA oligonucleotides	5′-GCCAGTCCAGCGTTTTTG-3′
Non-complementary DNA oligonucleotides	5′-ATTCCAATGTTACCGCCA-3′
Primer UAL-1939	5′-TATGGAATTTCGCCGATTTT-3′
Primer UAR-2105	5′-TGTTTGCCTCCCTGCTGCGG-3′
PCR product	5′-**TGTTTGCCTCCCTGCTGCGG**TTTTTCACCGAA GTTCATGCCAGTCCAGCGTTTTTGCAGCAGAAAA GCCGCCGACTTCGGTTTGCGGTCGCGGGTGAAGA TCCCCTTCTTGTTACCGCCAACGCGCAATATGCCT TGCGAGGTCGC**AAAATCGGCGAAATTCCATA**-3′

[a] The sequence of PCR products in bold represents the sequence of the primers. The sequence underlined is complementary to the probe.

Table 2
The maximum frequency response and reagent loading of neutravidin, biotinylated DNA probe and complementary DNA oligonucleotides onto the PQC electrodes.

	Neutravidin	Biotinylated DNA probe	Complementary ssDNA oligonucleotides
Normal PQC sensor			
Maximum frequency response[a] (ΔF_{sol}, Hz)	310	53	44
Repeatability (%R.S.D., $n = 5$)	3.2	3.9	4.2
Maximum loading[b] ($\times 10^{-11}$ mol cm^{-2})	1.36	2.43	2.21
Neutravidin/DNA probe binding ratio	1	1.76	
Nano-Ag-modified PQC sensor			
Maximum frequency response[a] (ΔF_{sol}, Hz)	556	162	146
Repeatability (%R.S.D., $n = 5$)	4.9	6.0	7.8
Maximum loading[b] ($\times 10^{-11}$ mol cm^{-2})	2.48	7.46	7.33
Neutravidin/DNA probe binding ratio	1	3.01	
Nano-Au-modified PQC sensor			
Maximum frequency response[a] (ΔF_{sol}, Hz)	350	82	67
Repeatability (%R.S.D., $n = 5$)	13.4	24.5	51

[a] Excessive neutravidin and biotinylated DNA probes were applied onto each of the PQC electrodes for measurement of the maximum frequency response.
[b] The maximum reagent loadings are calculated from the frequency shift (ΔF_{air}) according to the Sauerbrey equation based on the ratio of $\Delta F_{sol}/\Delta F_{air} = 2:1$.

1.36×10^{-11} mol cm^{-2}. Thus, the amount of neutravidin loaded onto nano-Ag-modified PQC electrode is 1.82 times higher than that of the normal PQC electrode.

To characterize the quality of the immobilized neutravidin layer at the nano-Ag/TiO_2/PQC electrode, the electrochemical impedance spectrum (EIS) is measured after neutravidin immobilization with the Nyquist plot shown in Fig. 1 (plot d). From the large increase in the magnitude of the arc upon neutravidin immobilization, the calculated R_{et} value reaches 72,902 Ω. The rapid increase in R_{et} upon immobilization of the non-conducting neutravidin layer is attributed to the escalation in the blockage of the ferricyanide/ferrocyanide reaction at PQC electrode surface and a rapid elevation in the coating resistance upon progressive increase in thickness of the coating layer.

A larger decrease in the frequency shift (ΔF_{sol}) is observed (Table 2) upon immobilization of biotin-DNA probe onto the nano-Ag-modified electrode as compared to normal PQC electrode (162 Hz vs. 53 Hz, respectively). The ΔF_{air} values for the biotin-DNA interaction is not measured, as drying of the neutravidin layer prior to biotin-DNA immobilization can denature neutravidin, giving rise to the absence of binding between biotin. Assuming the ratio between ΔF_{sol} and ΔF_{air} is constant with the same value ($\Delta F_{sol}/\Delta F_{air}$ = 2:1) as the immobilization of neutravidin (Caruso et al., 1998), the frequency shifts for ΔF_{air} due to the immobilization of biotin-DNA are estimated as 81 and 26 Hz for nano-Ag and normal PQC electrodes, respectively.

Based on the Sauerbrey equation, the loading of DNA probes onto nano-Ag and normal PQC electrode are calculated to be 7.46×10^{-11} and 2.43×10^{-11} mol cm^{-2}, respectively. Thus, the maximum biotinylated probe loading onto the nano-Ag-modified PQC sensor is 3.07 times that of the normal PQC electrode. As the maximum amount of neutravidin loaded onto the nano-Ag-modified PQC electrode is only 1.82 times higher than normal PQC electrode, the interaction between neutravidin and biotinylated probes are clearly enhanced when nano-Ag is used in the PQC sensing layer. The molar binding ratio between neutravidin and biotinylated probes is calculated to be 1:3.01 for nano-Ag-modified PQC electrode, which is higher than normal PQC electrode (1:1.76). The results indicate that the binding capacity of neutravidin to biotinylated DNA probes is increased by more than 71% using nano-Ag as compared to normal PQC sensor.

3.4. The performance and applicability of the PQC/DNA biosensor for E. coli detection in drinking water

The frequency shifts during sequential immobilization with neutravidin and biotinylated ssDNA probes prior to hybridization with the complementary DNA strand at the nano-Ag and normal PQC electrode are shown in Fig. 4. The introduction of nano-Ag onto the PQC electrode is clearly shown to cause a large frequency shift during the deposition of the neutravidin/biotinylated ssDNA probes, as well as during hybridization between the biosensor and the complementary ssDNA. The results on the maximum frequency response and loading of complementary ssDNA upon hybridization at the PQC/DNA biosensor are given in Table 2, showing a much higher sensitivity achieved using the nano-Ag coating. To compare the maximum molar loadings of complementary DNA (2.21×10^{-11} and 7.33×10^{-11} mol cm^{-2}) to biotinylated DNA probe (2.43×10^{-11} and 7.46×10^{-11} mol cm^{-2}) for normal PQC and nano-Ag PQC, respectively, very similar values are obtained, indicating that the 1:1 hybridization between biotinylated DNA probe and complementary DNA is close to 100% within experimental error.

The maximum loading of complementary DNA has increased from 2.21×10^{-11} to 7.33×10^{-11} mol cm^{-2} on normal PQC and nano-Ag-modified PQC sensor, respectively, giving rise to an enhancement factor of about 3.3 times of the maximum DNA loadings, which is close to the enhancement of 3.07 times of biotinylated probes loading at the nano-Ag-modified PQC electrode. Thus, the enhancing performance of the PQC/DNA biosensor is mainly due to the improvement of the binding between neutravidin and biotinylated probe as the result of using nano-Ag in the PQC sensor coating.

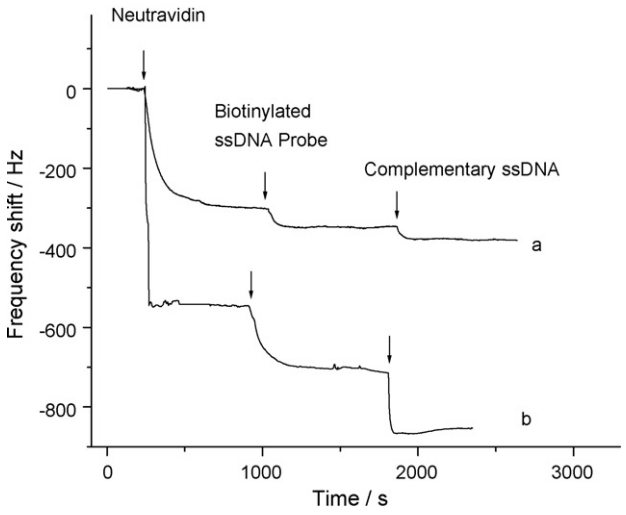

Fig. 4. Frequency responses of the PQC sensor in time sequence for electrode modification and subsequent detection of ssDNA: (a) normal PQC sensor; (b) nano-Ag-modified PQC sensor.

The enhancing of the signal response is attributed to the following effects arising from the nano-Ag coating. First, the use of nano-Ag particles produces a large increase in the active surface area at the sensor coating and a significant increase in the packing density of neutravidin. The combined effect give rises to an enhancement in the maximum neutravidin load to 1.8 times of a normal electrode. Second, the chemical interaction between the neutravidin with the surface of a freshly generated nano-silver layer activates the activity of the closely packed neutravidin layer (Ebersole et al., 1990; Burgess and Hawkridge, 1997; Jennings and Laibinis, 1996; Yan and Sadik, 2001). The activated neutravidin shows a higher functional activity to bind with biotinylated DNA probes, giving rise to an increase in the binding ratio between neutravidin and biotinylated DNA probes from 1.00:1.76 to 1.00:3.01. Third, the strong binding between neutravidin and biotinylated DNA probes improves the stability of the biotinylated DNA probes bounded to the sensor surface, giving rise to the enhancement in its subsequent hybridization with the complementary ssDNA. However, the method repeatability (Table 2) is slightly deteriorated as compared to normal PQC sensor (7.8% vs. 4.2% for complementary ssDNA oligonucleotides, respectively).

To be able to determine low counts of *E. coli* cells in water, efficient PCR amplification is needed. Considering the very low-*E. coli* counts in drinking water, 50 PCR cycles are performed. An increased number of cycles will not dramatically change the amount of products, as the amount of polymerase becomes a limiting factor in the presence of large copies of the target DNA (Molecular Cloning, 2008).

The biosensor fabricated was optimized to obtain the best analytical performance under flow analysis with online PCR products denaturing prior to PQC/DNA hybridization detection. To establish its working curve, a solution with highly amplified PCR products was quantified by UV spectrophotometry and diluted to different concentrations (0.0048–4800 μg/L) prior to recording their corresponding frequency shifts upon injection to the flow system for

online PCR products denaturing and PQC/DNA hybridization detection. The working curve was found to fit the following equation upon regression:

$$-\Delta F = 84 + 21 \log C \quad \text{with} \quad r = 0.9856$$

The detection limit based on 3 times signal to noise ratio is estimated to be 0.4 ng/L for PCR product and the repeatability (R.S.D., $n = 5$) at 9.8%. For testing the specificity of the PQC/DNA biosensor, negative control such as PCR blank and potential interferents such as genes from other bacteria and food sources (Hop D gene from *Helicobacter pylori* (0.001 mg/mL), PET 32a plasmid gene (0.001 mg/mL) and Calf thymus DNA (0.01 mg/mL)) have been investigated with results showing no significant interference as less than 10 Hz frequency shift has been observed. Thus, the specificity of the PQC/DNA biosensors developed to the complementary DNA from the PCR products of *E. coli* has been demonstrated.

The use of 10×10^6 *E. coli* cells (counted by flow cytometry) is shown to generate 48 μg/L products after 50 cycles of PCR amplification. Thus, to produce a detectable amount of 0.4 ng/L DNA PCR products, eight *E. coli* cells are needed before PCR amplification, which corresponds to the method detection limit in *E. coli* cell for nano-Ag-modified PQC sensor. For normal PQC biosensor, 23 bacterial cells can be consistently detected (Sun et al., 2006), indicating that the sensitivity has been improved by almost 3 times. Although the results based on PCR estimation is semi-quantitative, it is sufficient to indicate whether or not the present WHO guideline for drinking water quality is exceeded. According to the WHO guideline of drinking water quality, no *E. coli* cell should be detected in 100 mL water sample. Thus, the total volume of the tested water sample should be at least 800 mL in order to use the PQC/DNA biosensor developed to detect the presence of a single *E. coli* cell present in a 100 mL drinking water.

4. Conclusions

A highly sensitive PQC/DNA biosensor is developed to detect low level of *E. coli* in drinking water through signal amplification by photochemical deposition of nano-Ag at normal Au PQC electrode. A repeatable amount of nano-silver coating is obtained by photochemical deposition in 10^{-2} M $AgNO_3$ solution (10%, v/v methanol). The maximum loading of neutravidin (2.48×10^{-11} mol cm^{-2}) at freshly produced nano-Ag PQC is 1.82 times larger and the maximum biotinylated probe loading (7.46×10^{-11} mol cm^{-2}) on neutravidin/nano-Ag-modified PQC sensor 3.07 times that of an uncoated PQC electrode. The binding ratio between the neutravidin and biotinylated DNA probe is increased from 1.00:1.76 of normal PQC to 1.00:3.01 using the nano-silver-modified electrode, leading to an increase of more than 71% of the binding capacity of neutravidin to biotinylated DNA probes and an enhancement of 3.3 times for binding of complementary DNA onto the nano-Ag-modified neutravidin/biotinylated DNA PQC biosensor. The enhancement of detection sensitivity for binding complementary DNA is attributed to the following effects arising from the nano-Ag coating. First, the large increase in the active surface area and packing density of neutravidin lead to enhancement in the maximum neutravidin load. Second, the closely packed neutravidin activated by interaction with nano-Ag enhances its functional activity to bind biotinylated DNA probes, elevating the binding ratio from 1.00:1.76 to 1.00:3.01. Third, the stronger binding leads to a higher stability of the biotinylated DNA probes bound and increase in hybridization with the complementary DNA. Under the optimized conditions, a linear working curve of $-\Delta F = 84 + 21 \log C$ with $r = 0.9856$ for C in μg/L, and a detection limit of 0.4 ng/L for DNA PCR products (equivalent of eight *E. coli* cells) are obtained. The total volume of water sample should be at least 800 mL in order to detect a single *E. coli* cell in a 100 mL drinking water to satisfy the WHO requirement.

Acknowledgements

We would to thank Dr. S.P. Ng for discussion and the support from the Hong Kong Research Grants Council of the Hong Kong Special Administrative Region, China (HKU 7043/03P) and the Hong Kong University Research and Conference Grants Committee.

References

Arora, K., Prabhakar, N., Chand, S., Malhotra, B.D., 2007. Anal. Chem. 79 (6), 6152–6158.
Burgess, J.D., Hawkridge, F.M., 1997. Langmuir 13 (14), 3781–3786.
Caruso, F., Rodda, E., Furlong, D.F., Niikura, K., Okahata, Y., 1997. Anal. Chem. 69 (11), 2043–2049.
Caruso, F., Furlong, D.N., Niikura, K., Okahata, Y., 1998. Colloid. Surf. B 10 (4), 199–204.
Chen, H.W., Ku, Y., Kuo, Y.L., 2007. Chem. Eng. Technol. 30 (9), 1242–1247.
Chu, X., Zhao, Z.L., Shen, G.L., Yu, R.Q., 2006. Sens. Actuat. B 114 (2), 696–704.
Ebersole, R.C., Miller, J.A., Moran, J.R., Ward, M.D., 1990. J. Am. Chem. Soc. 112 (8), 3239–3241.
Friedmann, D., Hansing, H., Bahnemann, D., 2007. Int. J. Res. Phys. Chem. Chem. Phys. 221 (3), 329–348.
Fu, X.H., 2008. Bioprocess. Biosyst. Eng. 31 (2), 69–73.
Fu, Y.C., Xie, Q.J., Jia, X.E., 2007. J. Electroanal. Chem. 603 (1), 96–106.
Ghafouri, S., Thompson, M., 1999. Langmuir 15 (2), 564–572.
2004. Guideline Values for Drinking Water, 3rd ed. World Health Organization.
Hoshino, Y., Kawasaki, T., Okahata, Y., 2006. Biomacromolecules 7 (3), 682–685.
Hwang, E.S., Cao, C.F., Hong, S.H., Jung, H.J., Cha, C.Y., Choi, J.B., Kim, Y.J., Baik, S., 2006. Nanotechnology 17 (14), 3442–3445.
Iqbal, S., Robinson, J., Deere, D., Saunders, J.R., Edwards, C., Porter, J., 1997. Lett. Appl. Microbiol. 24, 498–502.
Jennings, G.K., Laibinis, P.E., 1996. Langmuir 12 (26), 6173–6175.
Kim, H., Kane, M.D., Kim, S., Dominguez, W., Applegate, B.M., Savikhin, S., 2007. Biosens. Bioelectron. 22 (6), 1041–1047.
Leung, P.H.M., Yam, W.C., Ng, W.W., Peiris, J.S., 2001. Epidemiol. Infect. 126 (2), 173–179.
Liu, T., Tang, J., Jiang, L., 2004. Biochem. Biophys. Res. Commun. 313 (1), 3–7.
Loaiza, O.A., Campuzano, S., Pedrero, M., Pingarron, J.M., 2007. Talanta 73 (5), 838–844.
Manso, J., Mena, M.L., Yanez-Sedeno, P., 2008. Anal. Biochem. 375 (2), 345–353.
Mao, X.L., Yang, L.J., Su, X.L., 2006. Biosens. Bioselectron. 21 (7), 1178–1185.
Molecular Cloning, 2008. In Vitro Amplification of DNA by the Polymerase Chain Reaction. Cold Spring Harborr Laboratory Press, http://www.molecularcloning.com.
Ogi, H., Motoshisa, K., Matsumoto, T., Hatanaka, K., Hirao, M., 2006. Anal. Chem. 78 (19), 6903–6909.
Raj, C.R., Abdelrahman, A.I., Ohsaka, T., 2005. Electrochem. Commun. 7 (9), 888–893.
Sauerbrey, G., 1959. Z. Phys. 155 (2), 206–222.
Shervedani, R.K., Bagherzadeh, M., 2008. Electroanalysis 20 (5), 550–557.
Sivanesan, A., Kannan, P., John, S.A., 2007. Electrochim. Acta 52 (28), 8118–8124.
Su, X.L., Li, Y.B., 2005. Biosens. Bioelectron. 21 (6), 840–848.
Sun, H., Zhang, Y.Y., Si, S.H., Zhu, D.R., Fung, Y.S., 2005. Sens. Actuat. B 108 (1–2), 925–932.
Sun, H., Zhang, Y.Y., Fung, Y.S., 2006. Biosens. Bioelectron. 22 (4), 506–512.
Tao, H., Wei, W.Z., Zhang, S.F., 2004. J. Photochem. Photobiol. A 161 (2–3), 193–199.
Wu, V.C.H., Chen, S.H., Lin, C.S., 2007. Biosens. Bioelectron. 22 (12), 2967–2975.
Yan, F., Sadik, Q.A., 2001. J. Am. Chem. Soc. 123 (46), 11335–11340.
Zhang, S.X., Wang, N., Yu, H.J., Niu, Y.M., Sun, C.Q., 2005. Bioelectrochemistry 67 (1), 15–22.
Zhong, Z.Y., Patskovskyy, S., Bouvrette, P., Luong, J.H.T., Gedanken, A., 2004. J. Phys. Chem. B 108 (13), 4046–4052.